SECED 2023 Conference
Earthquake Engineering & Dynamics for a Sustainable Future
14-15 September 2023, Cambridge, UK

A METHODOLOGY FOR THE RISK-BASED DESIGN OF BRIDGES IN ITALY

Francesca TURCHETTI[1], Enrico TUBALDI[2], John DOUGLAS[3], Mariano ZANINI[4] & Andrea DALL'ASTA[5]

Abstract: *Seismic design codes used worldwide are mainly based on a force-based seismic design approach, employing Uniform-Hazard Spectra (UHS) to select the seismic action and behaviour factors to account for the inelastic behaviour of structures. Lately, following the increasing interest in performance-based earthquake engineering, many studies investigated the reliability of this design approach by assessing the level of structural safety against earthquake actions implicitly achievable following design codes. It emerged that current code provisions do not ensure a uniform level of structural safety. For the abovementioned reasons, the present contribution assesses the seismic structural safety of newly-designed bridges in Italy. In particular, the study proposes a methodology for the risk-targeted design of reinforced concrete piers in multi-span bridges. Such an approach consists in computing the probability of failure of the structure by solving a direct reliability problem, associated with the exceedance of tolerable thresholds of loss. The methodology is applied in various locations across Italy to illustrate the variations in the optimal risk-based design properties of bridges across regions with varying seismic hazard.*

Introduction

The seismic design of structures recommended by current seismic codes relies on a simplified approach that employs Uniform Hazard Spectra (UHS) to determine the seismic action (e.g. Gkimprixis et al. 2020). Following the development of modern performance-based earthquake engineering, many studies have shown that a major drawback of this simplified design approach is the inability to ensure a sufficient and uniform level of structural safety against earthquake actions for different structural archetypes located at various sites (e.g. Cornell and Krawinkler 2000, Tubaldi et al. 2012). Over the past decade, risk-targeted seismic design emerged as one of the most promising approaches for designing structures with controlled seismic risk and/or loss levels.

Following the work of Luco et al. (2007), the principle of "risk-targeting" has been embedded in the development of design maps that are currently used in US design codes (e.g. ASCE/SEI 7-10 2013). As discussed by Fajfar (2018), the risk-targeting paradigm and concepts of risk-targeted maps and behaviour factors (Žižmond and Dolšek 2019) are expected to form the basis of future design codes for many countries (Douglas and Gkimprixis 2018). While most of the studies and codes focus on the design of buildings, risk-targeted bridge design is a less explored topic. Wang et al. (2014) proposed a method to design reinforced concrete (RC) bridge columns to achieve a uniform risk of failure. Deb et al. (2022) proposed a method for risk-targeted performance-based seismic design of bridge piers for Californian Ordinary Standard Bridges to facilitate risk-informed design and decision making.

The present study proposes a simplified risk-targeted method for the seismic design of RC piers in multi-span bridges. The only design variables considered are the pier diameter and the longitudinal reinforcement ratio. A meta-model is built to describe the changes in the bridge seismic fragility with these two design parameters. The optimal values of the design parameters are found as the solution of a simplified reliability-based optimization problem, for which it is not necessary to resort to time-consuming optimization strategies. The methodology is applied in

[1] PhD student, University of Strathclyde, Glasgow, UK, francesca.turchetti@strath.ac.uk
[2] Senior Lecturer, University of Strathclyde, Glasgow, UK
[3] Senior Lecturer, University of Strathclyde, Glasgow, UK
[4] Assistant Professor, University of Padova, Padova, Italy
[5] Professor, University of Camerino, Ascoli Piceno, Italy

various locations across Italy to illustrate the variations in the optimal risk-based design properties of bridges across regions with varying seismic hazard.

Risk-targeting design procedure

The assessment of the bridge risk and the design of the bridge properties that satisfy a prefixed performance level are evaluated via direct and inverse reliability problems. Similar to Wang et al. (2014) and Deb et al. (2022), the risk-targeted design problem for a single bridge pier is considered. This simplification is introduced due to the role played by bridge piers in controlling the seismic behaviour of bridges and also to facilitate the illustration of the proposed risk-based design procedure.

Direct problem

The design procedure proposed herein is based on the solution of the direct reliability problem, which consists in evaluating the probability of exceeding one (or more) limit state(s) of interest in the time interval of interest. As discussed in Scozzese et al. (2020), an intensity-measure (*IM*)-based approach is employed. A capacity/demand format is used to evaluate the limit-state exceedance probability given the seismic intensity. The capacity is measured by a positive real-valued random variable *C*, whose possible realizations are denoted by *c*, with probability density function (PDF) $f_C(c)$ and cumulative density function (CDF) $F_C(c)$. The demand *D* is also expressed as a positive real valued random variable, whose possible realizations are denoted by *d*. The conditional distribution of the demand following events with a seismic intensity *im* is described by $f_{D|IM}\left(d|im\right)$. The probability of failure associated to the condition *C<D* conditional to *IM=im* is:

$$P_{f|IM}\left(im\right) = \int F_C\left(z\right) f_{D|IM}\left(z|im\right) dz \tag{1}$$

where *z* is a dummy variable. It is assumed that an event such that *IM>im* can be described by a Poisson process fully defined by the Mean Annual Frequency (MAF) $v_{IM}(im)$. Under the assumptions that the probability distribution of the earthquake characteristics remains the same at each earthquake occurrence, and so does the probability of exceedance of the limit state, the probability of failure per year (failure rate) coincides with the MAF of failure and can be evaluated as follows:

$$v_f = \int_{im} P_{f|IM}\left(im\right) \cdot \left|\mathrm{d}v_{IM}\left(im\right)\right| \tag{2}$$

The probability of failure in a time interval, e.g. the expected design lifetime t_L, can be obtained as:

$$P_{f,t_L} = 1 - e^{-\nu_f \cdot t_L} \tag{3}$$

The capacity is assumed as a log-normal random variable and the two parameters associated to this distribution, the median $\hat{c}$ and the standard deviation of the logarithms β_C, are known and independent of the *IM*. It is also assumed that the demand conditional on the seismic intensity is a log-normal random variable, with parameters $\hat{d}$ and β_D. The relationship between *IM* and *D* can be expressed as:

$$\log\left[D|IM = im\right] = \log\left[\hat{d}\left(im\right)\right] + \varepsilon = a + b \cdot \log\left(im\right) + \varepsilon \tag{4}$$

where ε is a normally distributed random variable with zero mean and standard deviation β_D. The three parameters *a, b* and β_D can be determined through ordinary least squares regression. In this study, cloud analysis is carried out to develop the probabilistic seismic demand model (Jalayer 2003). The conditional probability of failure can be expressed in a closed form as:

$$P_{f|IM}\left(im\right) = \Phi\left[\frac{\log\left[\hat{d}\left(IM\right)/\hat{c}\right]}{\sqrt{\beta_D^2 + \beta_C^2}}\right] \tag{5}$$

and the MAF of failure can be evaluated by Eqn. (2) once the MAF of *im* is assigned.

Inverse problem

Let **x** $\in R^n$ denote the vector of design parameters (e.g. pier longitudinal reinforcement ratio and pier diameter). The risk-targeted design of bridges is an inverse reliability problem that can be cast in the form of an optimization problem: find the set of optimal design parameters **x*** such that an objective function (cost function) is minimised. The solution must satisfy a stochastic constraint requiring that the failure probability (or the MAF of failure) is less or equal to a pre-fixed value, as well as other constraints on the values that can be assumed by **x**. In mathematical terms, the problem can be formalised as follows:

$$\begin{aligned} \min_{\mathbf{x}} \quad & g(\mathbf{x}) \\ \text{subject to} \quad & \mathbf{h}(\mathbf{x}) \leq 0 \\ & \nu_f(\mathbf{x}) - \bar{\nu}_f \leq 0 \end{aligned} \tag{6}$$

where $g(\mathbf{x})$ is a cost function, depending on the design parameters, and $\mathbf{h}(\mathbf{x})$ is the set of constraints on the range of variation of **x**. In Eqn. (6), the dependency of the MAF of failure on the design parameters **x** has been made explicit. The choice of a suitable cost function is essential for ensuring that a single design point is obtained. In fact, various combinations of the design parameters ensure that $\nu_f(\mathbf{x}) - \bar{\nu}_f \leq 0$.

Design procedure

The reliability-based design procedure for this problem consists of the following steps:

1. Select various combinations of the design parameters DPs. These could be arranged to form a design of experiments matrix $\boldsymbol{X}_E = [\mathbf{x}_1 \cdots \ \mathbf{x}_j \cdots \ \mathbf{x}_{N_E}] \in R^{n \times N_E}$, where $\mathbf{x}_j = [x_{1j} \quad x_{2j} \quad x_{nj}]^T \in R^n$ denotes the vector corresponding to the *j*-th combination of design parameters, and N_E denotes the total number of design points;

2. For each combination of the DPs, the design flexural resistance M_{Rd} of the plastic hinge section at the base of the pier is derived in accordance with Eurocode 8 provisions (CEN EN 1998-1:2004). Subsequently, the transverse reinforcement is designed by applying capacity design principles (CEN EN 1998-1:2004); the confined concrete properties in the plastic hinge are evaluated using the Mander et al. (1988) model and a nonlinear FE model of the bridge is developed;

3. Cloud analysis is performed to develop a probabilistic demand model for the EDPs of interest. In this study, a single limit state, corresponding to the exceedance of the ductility capacity of the bridge, is considered. This is likely to be the most critical failure mode in newly designed bridges, because the application of capacity design principles ensures that the probability of occurrence of other failure modes (e.g. shear failure) is negligible.

4. Thus, the monitored EDP is the displacement demand at the pier top, which must be compared to the displacement capacity;

5. The probability $P_{f|IM}(im, \mathbf{x}_E)$ of exceedance of the limit state of interest conditional to the chosen *IM* and the combination of DPs in $\mathbf{x}_E$ is evaluated;

6. Based on the values of the conditional failure probability evaluated in correspondence of the support points, a surrogate model is fitted that provides the conditional failure probability for any possible value of **x** without needing to perform other seismic response analyses. The simplest approach for developing the surrogate model is to use linear interpolation;

7. Given a site of interest, characterized by a hazard curve $\nu_{IM}(im)$, the MAF of failure given **x**, $\nu_f(\boldsymbol{x})$, can be evaluated and used to solve the problem formalised in Eqn. (6).

Cost function

The form adopted for the optimization problem is such that the consequences of pier failure in terms of direct and indirect losses are controlled by setting a maximum value of the MAF of failure. Since the total bridge life cycle cost is the sum of the cost of bridge construction and the cost due to failure, in order to minimise this cost one could consider the pier cost as the cost function. The cost function is assumed to coincide with the design resisting moment at the base of the pier, M_{Rd}. This quantity is expected to be correlated to the bridge construction cost, as it increases with the pier diameter, the amount of longitudinal reinforcement, the concrete class and other factors. Moreover, by minimising M_{Rd} the design shear (and thus the amount of transverse reinforcement) is also minimised.

Target failure probability

The minimum values of the reliability index for a reference period of 1 year, recommended in Eurocode 0 (CEN EN 1990:2002), should be 4.2 for consequence class CC1 structures, 4.7 for CC2 class structures and 5.2 for CC3 class structures. These correspond respectively to a MAF of failure of 1.33×10^{-5} years^{-1}, 1.33×10^{-6} years^{-1} and 9.96×10^{-8} years^{-1}. However, it is not clear whether the values should be considered for the seismic design, as the draft version of the revised Eurocode 0 explicitly exclude these (Fajfar 2018). Appendix F of the draft version of the revised Eurocode 8 (Dolsěk et al. 2017b) suggests a target of 2×10^{-4} years^{-1}, which according to Fajfar (2018) is a value comparable to the probabilities of failure estimated for buildings compliant with current seismic codes. Many studies have adopted the US target value of $2\text{x}10^{-4}$ without much discussion, although Douglas et al. (2013) conclude that a target of $1\text{x}10^{-5}$ or even $1\text{x}10^{-6}$ would be easier to justify based on risk targets from other fields such as nuclear safety. Using a database of collapsed RC buildings in Italy and Greece over the previous few decades, Douglas and Gkimprixis (2018) conclude that the observed risk of collapse for such structures is between 1×10^{-6} and 1×10^{-5}. Because of the importance of road bridges both for life safety and their economic impact during and following earthquakes, a target MAF of failure of 1×10^{-6} is adopted for the following case study. The effect of this choice is examined by also considering 1×10^{-5} and $2\text{x}10^{-4}$ in subsequent steps.

Case study description and results of parametric analyses

The case study used to illustrate the application of the proposed design method is represented by a two-span bridge with a continuous multi-span deck. The RC pier is 5.4m high and has a circular cross-section with diameter D_p. The three-dimensional FE model of the bridge is developed in OpenSees (2011) using the beam element with inelastic hinge developed by Scott et al. (2006) to describe the bottom of the pier, and linear elastic elements to describe the remaining part of the pier. The elastic damping properties of the system are characterized by a Rayleigh damping model. The same bridge is assumed to be located at various sites in Italy, characterized by different seismic hazards. The only DPs herein considered are the pier diameter D_p and the longitudinal reinforcement ratio ρ_L; thus $\mathbf{x}=[D_p, \rho_L]$. These DPs are assumed to vary in a realistic range that reflects construction practice and satisfies code requirements. In particular, the values of D_p of 1.4m, 1.8m, and 2.2m and the values of ρ_L of 1%, 2%, 3% and 4% are considered. For simplicity, two-dimensional linear interpolation is used to find the values of dependent variables corresponding to intermediate values of D_p and ρ_L.

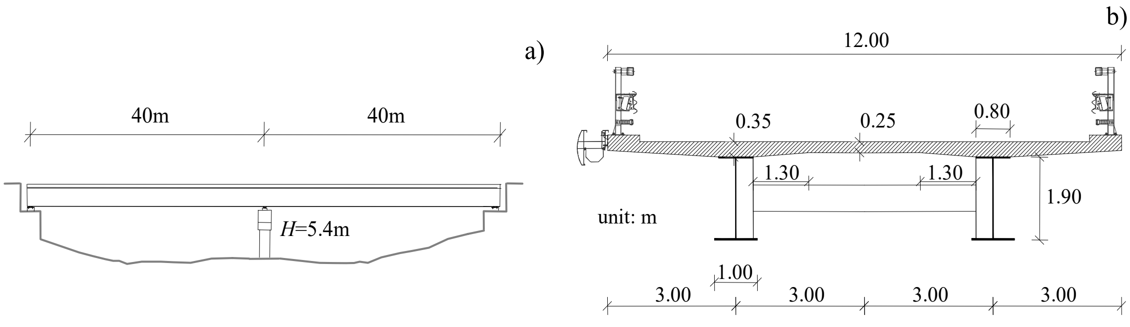

Figure 1: a) Two-span bridge profile, b) transverse deck section (source Tubaldi et al. (2013)).

Probabilistic seismic demand models (PSDMs) are developed for the various design cases after performing cloud analysis. For this purpose, the same ground motion records employed in Tubaldi et al. (2022) is used. The maximum top displacements $u_{max,L}$ and $u_{max,T}$ along the longitudinal and transverse direction are considered to develop the PSDM. The intensity measure considered is $RotD50Sa_{avg}$, which is obtained as follows: first, the *RotD50* (Boore 2010) of the pseudo-acceleration response spectrum for the 221 records (two horizontal components) is computed, for a series of periods in the range between 0.1s and 2.5s, and for a 5% damping ratio. Then, the geometric mean of these is evaluated to obtain the $RotD50Sa_{avg}$. It is noteworthy that the proposed *IM* is not structure-specific.

Figure 2 shows the fragility curves for the various combinations of DPs. It can be observed that both the diameter and the longitudinal reinforcement ratio significantly affect the bridge fragility. Overall, increasing D_p is more effective than increasing ρ_L in reducing the bridge fragility. However, increasing the reinforcement ratio has a more significant effect in terms of reduction of fragility for large pier diameters than for low ones.

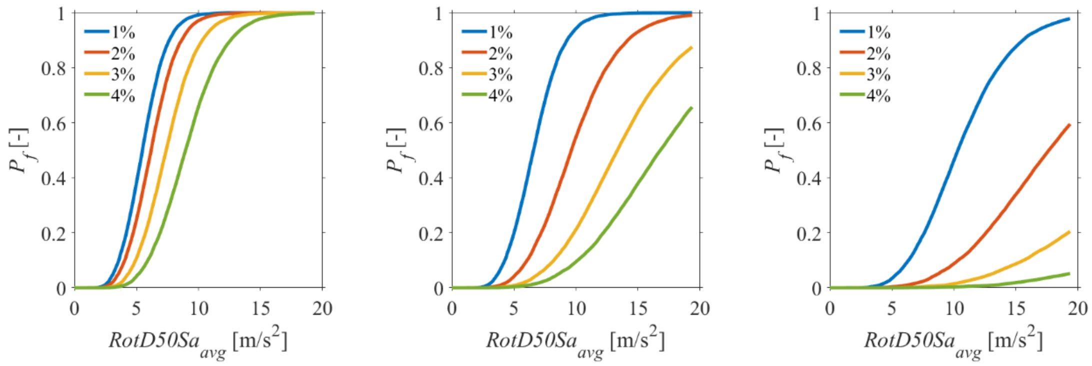

(a) (b) (c)

Figure 2: Fragility curves for different combinations of DPs (a) D_p =1.4m (b) D_p =1.8m (c) D_p=2.2m.

Results of the risk-targeting design approach

Probabilistic seismic hazard assessment (PSHA) is carried out on a regular grid spaced by 0.05° for Italy. The hazard curves for each site have been built using the software REASSESS V2.0 (Chioccarelli et al. 2019), using the ground motion prediction equation proposed by Lanzano et al (2019) for *RotD50Sa*. The seismogenic source model is the one proposed by Meletti et al. (2008) with parameters taken from Barani et al. (2009). The interval of interest of the selected *IM* values ranges between 10^{-5}g and +2g. The condition of "Soil Type A" has been considered.

Figure 3a shows hazard curves in terms of MAF of exceedance of different values of $RotD50Sa_{avg}$ for three Italian cities: Milan, Naples and L'Aquila. The three sites are exposed to roughly low-, mid-, and high-seismic hazard. Figure 3b compares the MAFs of bridge pier failure corresponding to the minimum values of DPs (in green), and to the maximum values of DPs (in grey) for the three considered sites.

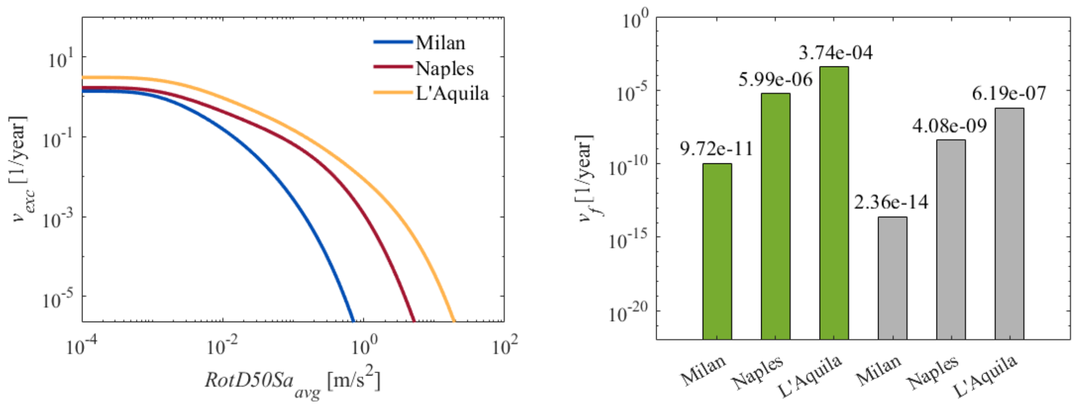

(a) (b)

Figure 3: (a) Comparison of hazard curves in terms of RotD50Saavg for three different sites in Italy; (b) comparisons of risks for ρ_L =1%, D_p =1.4m in green and ρ_L =4%, D_p =2.2m in grey.

Figure 4 shows the values of the design resisting moment M_{Rd} at the pier base. It can be noted that increasing D_p and ρ_L results in an increase of M_{Rd}. In general, the design resisting moment is more sensitive to D_p than to ρ_L for low D_p values. However, for high D_p values increasing ρ_L results in large increase of M_{Rd}. In the same plot, the optimal design point (denoted by a star) and other combinations of DPs (marked with circles) satisfying the stochastic constraint of a MAF of failure equal or less than 10^{-6} are also shown. In particular, Figure 4a reports the results for a bridge located in L'Aquila. It can be observed that only one DP combination satisfies the required stochastic constraint in L'Aquila. Figure 4b shows the results for a bridge located in Naples. In this case, there are various combinations of DPs that satisfy the constraint on the acceptable risk of failure. Among these, the one that minimizes the resisting moment corresponds to D_p =1.4m and ρ_L =3.5%.

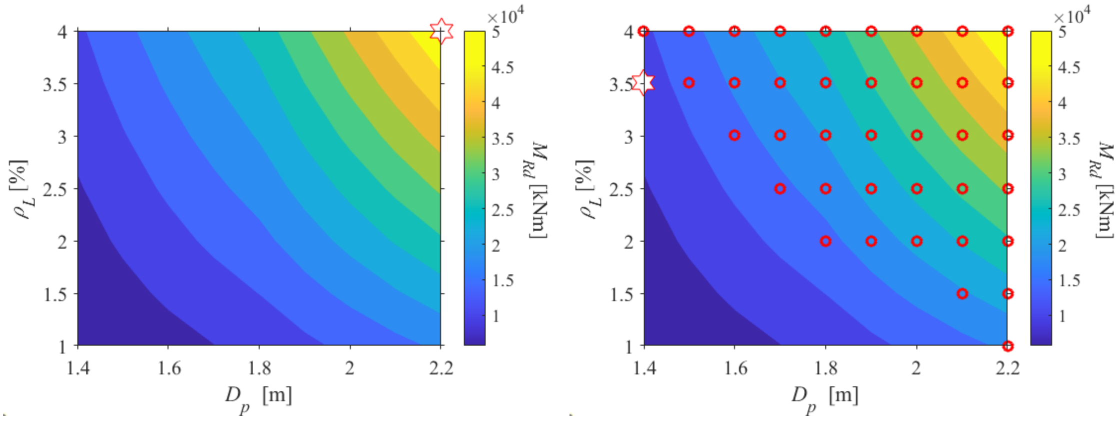

(a) (b)

Figure 4: Values of the resisting moment M_{Rd} for different combinations of DPs for a bridge site (a) in L'Aquila and (b) in Naples. The design parameters satisfying the stochastic constraint are marked with a circle, the optimal design point is marked by a star.

Figure 5a shows the variation of the MAF of failure with the design resisting moment M_{Rd} for the site of L'Aquila. It can be observed that there is a strong and inverse correlation between these two quantities. A similar trend is observed for the case of Naples, illustrated in Figure 5b.

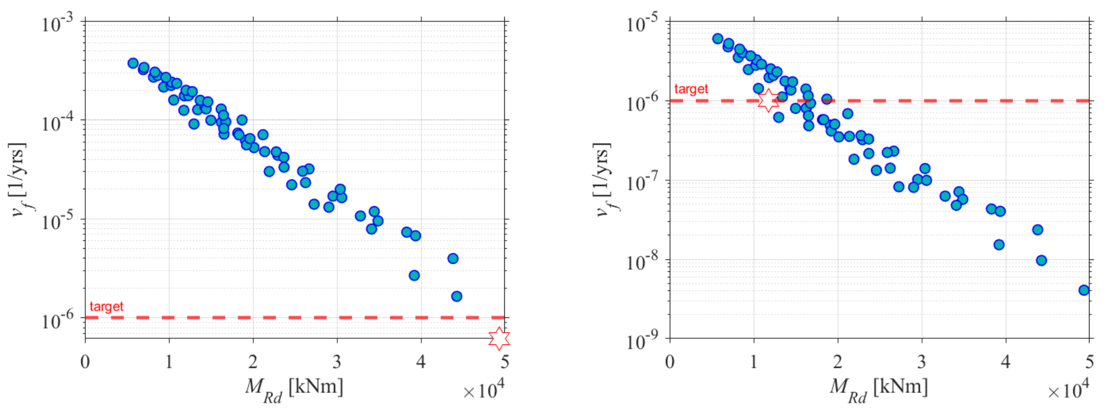

(a) (b)

Figure 5: Variation of the MAF of collapse vs. design resisting moment M_{Rd} obtained for various DP combinations for a bridge site in (a) L'Aquila and (b) Naples. The dashed red line indicates the target MAF of failure of 10^{-6} and the optimal design point is marked by a star. Note that the y-scale is different in the two plots.

Risk-based design maps for Italy

This section presents the results of the application of the proposed risk-targeting design procedure to the design of bridge pier across Italy. The target MAF of failure considered is 10^{-6}. Figure 6 shows the variation of minimum resisting moment M_{Rd} at the base of the pier across Italy, corresponding to the optimal design point. In large parts of Italy the minimum value of M_{Rd}, corresponding to ρ_L =1%, D_p =1.4m, is sufficient to satisfy the constraint and achieve risk levels less than 10^{-6}.

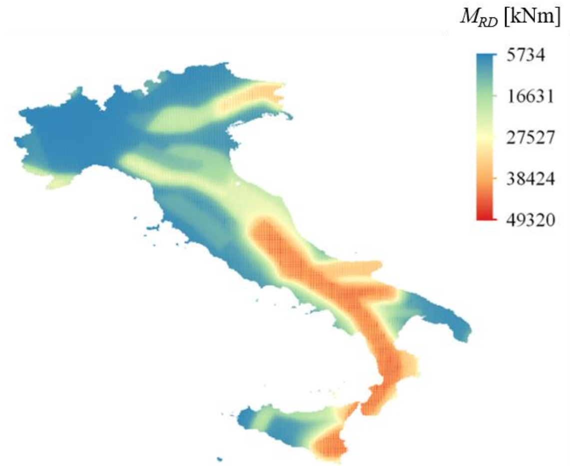

Figure 6: Variation across Italy of the minimum resisting moment M_{Rd} at the base of the pier.

Figure 7a and Figure 7b show a map of the optimal values of the pier diameter D_p and of the longitudinal reinforcement ratio ρ_L. In regions with lowest seismicity, the optimal DPs coincide with the minimum values of D_p and ρ_L, whereas in the regions with highest seismicity, they coincide with the maximum ones, as expected. Non-smooth changes of optimal DP values can be observed across adjacent regions that are characterized by quite similar levels of hazard. This is because high values of D_p and low values of ρ_L yield similar risk levels to low values of D_p and higher values of ρ_L. Obviously, a smoother variation of the optimal pier properties can be obtained if a single design parameter is considered, by keeping the other one fixed. Figure 8a shows the optimal values of ρ_L obtained considering a fixed diameter D_p of 2.2m. In this case, ρ_L exhibits a smooth variation across the country.

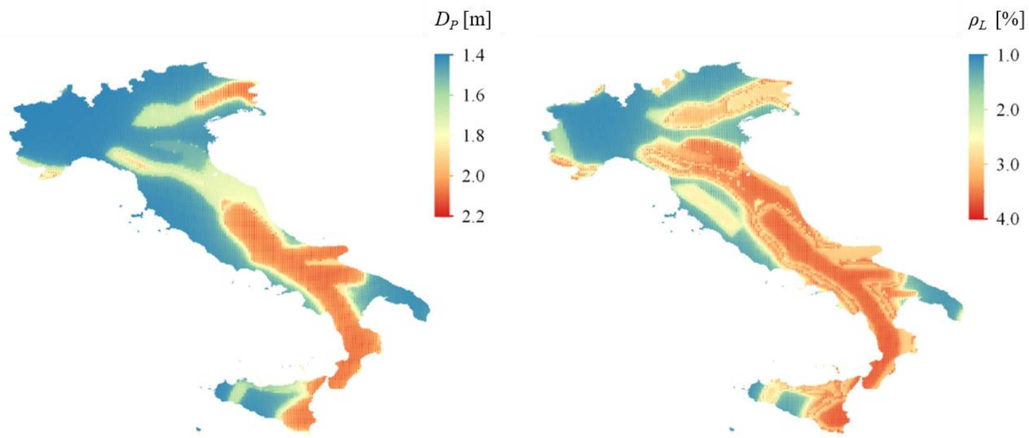

(a) (b)

Figure 7: Variation across Italy of the optimal pier diameter D_p (a) and of the optimal ρ_L (b).

The effect of the choice of the target risk level on the design parameters is evaluated by applying the proposed design procedure for a target MAF of failure of 10^{-5}. The results obtained for a fixed value of the pier diameter D_p = 2.2m are shown in Figure 8b. As expected, increasing the target risk level results in a significant reduction of the longitudinal reinforcement ratio across Italy.

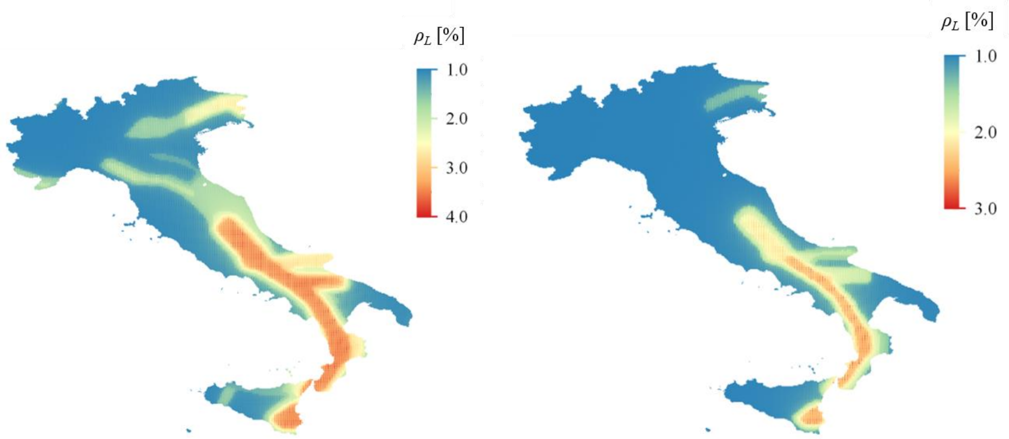

(a) (b)

Figure 8: Variation of the optimal ρ_L across Italy for D_p =2.2m obtained considering a target MAF of failure of 10^{-6} (a) and 10^{-5} (b).

The application of a MAF of failure of $2x10^{-4}$ is presented in Figure 9. In this case, as shown in Figure 9a, the highest value of the M_{Rd} is around 12000 kNm, corresponding to a longitudinal reinforcement ratio ρ_L of 4% and D_p=1,4 m. The minimum D_p is sufficient all over Italy while it is necessary to increase the amount of ρ_L in the southern regions with highest seismic hazard (Figure 9b).

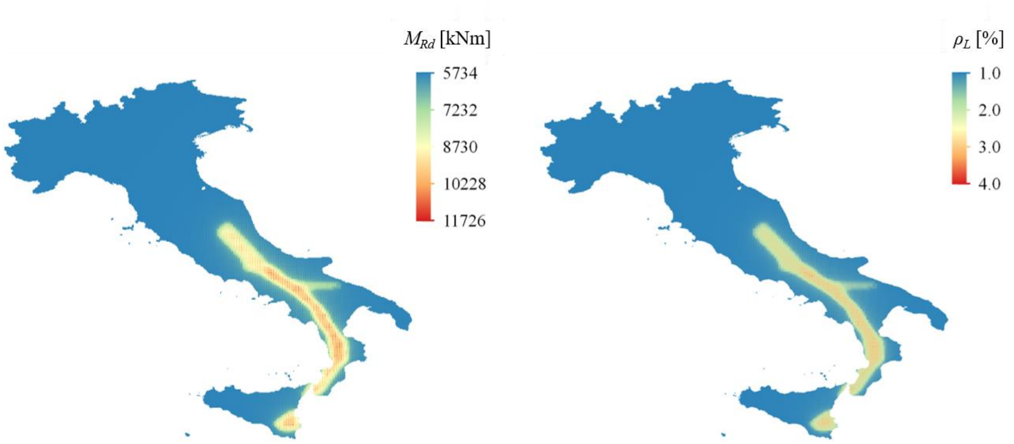

(a) (b)

Figure 9: Variation across Italy of the M_{Rd} at the base of the pier (a) and of the optimal ρ_L (expressed in terms of percentage) obtained considering a target MAF of failure of $2x10^{-4}$.

To provide insight into the effect of soil class on the application of the risk-targeting design procedure, the seismic hazard is assessed at the three sites previously considered (Milan, Naples and L'Aquila) for the soil types B, C and D. The new hazard curves are obtained using the software REASSESS V2.1 (Chioccarelli et al 2019) and using the same ground motion prediction equation adopted for soil type A. Figure 10 shows the new hazard curves for the three cities computed for soil B, C and D respectively whilst Table 1 reports the corresponding risk levels for two different combinations of design parameters. It can be observed that the increase of risk is highest for Milan and lowest for L'Aquila. Furthermore, the MAF of failure for the case of L'Aquila is above 10^{-6} even for the case of ρ_L =4%, D_c =2.2m and it is above 10^{-5} if soil D is considered. Thus, the soil type can have a considerable impact on the results of the risk-targeting design procedure.

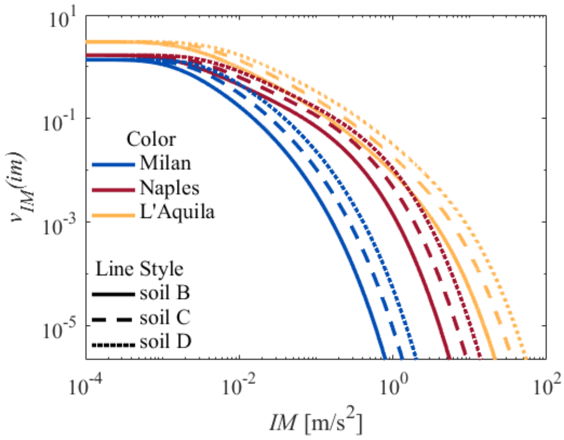

Figure 10: Comparison of hazard curves in terms of IM=RotD50Sa$_{avg}$ for three different sites in Italy assuming different soil classes.

	Milan		Naples		L'Aquila	
	D_p =1.4m ρ_L =1%	D_p =2.2m ρ_L =4%	D_p =1.4m ρ_L =1%	D_p =2.2m ρ_L =4%	D_p =1.4m ρ_L =1%	D_p =2.2m ρ_L =4%
Soil B	4.75e-10	2.36e-13	1.39e-05	1.36e-08	6.26e-04	1.96e-06
Soil C	1.18e-08	7.79e-12	9.50e-05	1.19e-07	1.81e-03	8.59e-06
Soil D	1.25e-07	9.47e-11	3.67e-04	6.17e-07	3.77e-03	2.35e-05

Table 1. Risks computed for Milan, Naples and L'Aquila for two combinations of DPs ([1.4,1%] and [2.2, 4%]) and for different soil classes.

Conclusions

The work presents a risk-targeting design procedure for bridge piers. The procedure identifies the optimal values of the pier diameter and longitudinal reinforcement ratio that minimise the resisting moment at the pier base while satisfying the stochastic constraint on the MAF of failure due to the exceedance of the pier displacement ductility capacity. Based on the obtained results, the following main conclusions can be drawn:

- The design resisting moment at the base of the pier exhibits a significant inverse correlation with the target MAF of failure and can be used to define the objective (cost) function to be minimised;
- Targeting values of the mean annual frequency of failure lower than 10^{-6} years^{-1} in regions of high seismicity requires design parameters that are out of the investigated range;
- A large variation of the optimal design parameters is observed across Italy, as a result of significant variations in the seismic hazard.
- In large parts of Italy, the minimum longitudinal reinforcement according to Eurocode 8 is sufficient to guarantee a target mean annual frequency of failure below 10^{-5} years^{-1}.
- The site classification can influence the design results, especially in regions of high seismicity. Design maps should be built for different soil types to better estimate the effect of the site classification.

References

ASCE (2013) Minimum design loads for buildings and other structures. ASCE/SEI 7-10.

Barani S, Spallarossa D, Bazzurro P. (2009) Disaggregation of probabilistic ground-motion hazard in Italy. *Bulletin of the Seismological Society of America*; 99:2638–2661

Boore, D. M. (2010) Orientation-independent, nongeometric-mean measures of seismic intensity from two horizontal components of motion, *Bulletin of the Seismological Society of America*.;100(4),1830–1835

CEN (2002) EN 1990:2002 + A1 Eurocode—basis of structural design. European Committee for Standardization, Brussels

CEN (2004) EN 1998-1:2004 Eurocode 8: design of structures for earthquake resistance—part 1: general rules, seismic actions and rules for buildings. European Committee for Standardization, Brussels

Chioccarelli, E., Cito, P., Iervolino, I., & Giorgio, M. (2019) REASSESS V2. 0: software for single- and multi-site probabilistic seismic hazard analysis. *Bulletin of Earthquake Engineering*;17(4), 1769-1793

Cornell, C. A., and H. Krawinkler. (2000) Progress and challenges in seismic performance assessment. *PEER Center News*,

Deb, A., Zha, A. L., Caamaño-Withall, Z. A., Conte, J. P., & Restrepo, J. I. (2022) Simplified Risk-Targeted Performance-Based Seismic Design Method for Ordinary Standard Bridges. *Journal of Bridge Engineering*; 27(10), 04022089

Dolsˇek M, Z ˇ izˇmond J, Kosicˇ M, Lazar Sinkovic´ N. (2017b) Simplified reliability-based verification format, working material for Annex F to revised EN 1998-1. University of Ljubljana, Ljubljana

Douglas J., Ulrich T., (2013) Negulescu C. Risk-targeted seismic design maps for mainland France. *Nat Hazards*;65, 1999-2013.

Douglas, J., Gkimprixis, A. (2018) Risk targeting in seismic design codes: the state of the art, outstanding issues and possible paths forward. *Seismic hazard and risk assessment*; 211-223

Fajfar, P. (2018) Analysis in seismic provisions for buildings: past, present and future. *Bull Earthquake Eng*; 16, 2567–2608.

Gkimprixis, A., Tubaldi, E., & Douglas, J. (2020) Evaluating alternative approaches for the seismic design of structures. *Bull Earthquake Eng*; *18*(9): 4331-4361.

Jalayer F. Direct Probabilistic Seismic Analysis: Implementing Nonlinear Dynamic Assessments. Stanford University; 2003

Lanzano, G., Luzi, L., Pacor, F., Felicetta, C., Puglia, R., Sgobba, S., D'Amico, M. (2019) A Revised Ground-Motion Prediction Model for Shallow Crustal Earthquakes in Italy. *Bulletin of the Seismological Society of America* ;109, 525–540

Luco, N., Ellingwood, B. R., Hamburger, R. O., Hooper, J. D., Kimball,J. K., and Kircher, C. A. (2007) Risk-targeted versus current seismic design maps for the conterminous United States. Proc., SEAOC2007 Convention, Structural Engineers Association of California, Sacramento, CA

Mander JB, Priestley MJN, Park RJ. (1988) Theoretical stress–strain model for confined concrete. *Journal of Structural Engineering*;114(8):1804–25

Meletti C, Galadini F, Valensise G, Stucchi M, Basili R, Barba S, Vannucci G, Boschi E (2008) A seismic source zone model for the seismic hazard assessment of the Italian territory. *Tectonophysics*; 450:85–108

OpenSees, the open system for earthquake engineering simulation. Pacific Earthquake Engineering Research Centre. Berkeley: University of California; 2011

Scott, M., Fenves, G. (2006) Plastic Hinge Integration Methods for Force-Based Beam-Column. Elements. *Journal of Structural Engineering-asce*; 132(2),244-252.

Tubaldi, E., Barbato, M., & Ghazizadeh, S. (2012) A probabilistic performance-based risk assessment approach for seismic pounding with efficient application to linear systems. *Structural Safety*;*36*, 14-22

Tubaldi, E., Dall'Asta, A., Dezi, L. (2013) Reduced formulation for post-elastic seismic response of dual load path bridges. *Engineering structures*;51, 178-187.

Tubaldi, E., Ozer, E., Douglas, J., & Gehl, P. (2022) Examining the contribution of near real-time data for rapid seismic loss assessment of structures. *Structural Health Monitoring*; 21(1), 118-137.

Wang, Z., Padgett, J. E., & Dueñas-Osorio, L. (2014) Toward a uniform seismic risk design of reinforced concrete bridges: A displacement-based approach. *Structural safety*; 50, 103-112.

Žižmond J., Dolšek M. (2019) Formulation of risk-targeted seismic action for the force-based seismic design of structures. *Earthq Eng Struct Dynam*;48(12): 1406-1428.